Crystal Structures of *Escherichia coli* Dihydrofolate Reductase Complexed with 5-Formyltetrahydrofolate (Folinic Acid) in Two Space Groups: Evidence for Enolization of Pteridine O4[†,‡]

Hyunsook Lee,[§] Vicente M. Reyes,*[,||] and Joseph Kraut

Department of Chemistry and Biochemistry, University of California, San Diego, La Jolla, California 92093-0506

Received January 4, 1996; Revised Manuscript Received April 1, 1996[⊗]

ABSTRACT: The crystal structure of *Escherichia coli* dihydrofolate reductase (ecDHFR, EC 1.5.1.3) as a binary complex with folinic acid (5-formyl-5,6,7,8-tetrahydrofolate; also called leucovorin or citrovorum factor) has been solved in two space groups, $P6_1$ and $P6_5$, with, respectively, two molecules and one molecule per asymmetric unit. The crystal structures have been refined to an *R*-factor of 14.2% at resolutions of 2.0 and 1.9 Å. The $P6_1$ structure is isomorphous with several previously reported ecDHFR binary complexes [Bolin, J. T., Filman, D. J., Matthews, D. A., Hamlin, R. C., & Kraut, J. (1982) *J. Biol. Chem. 257,* 13650−13662; Reyes, V. M., Sawaya, M. R., Brown, K. A., & Kraut, J. (1995) *Biochemistry 34,* 2710−2723]; enzyme and ligand conformations are very similar to the $P6_1$ 5,10-dideazatetrahydrofolate complex. While the two enzyme subdomains of the $P6_1$ structure are nearly in the closed conformation, exemplified by the methotrexate $P6_1$ binary complex, in the $P6_5$ structure they are in an intermediate conformation, halfway between the closed and the fully open conformation of the apoenzyme [Bystroff, C., Oatley, S. J., & Kraut, J. (1990) *Biochemistry 29,* 3263−3277]. Thus crystal packing strongly influences this aspect of the enzyme structure. In contrast to the $P6_1$ structure, in which the Met-20 loop (residues 9−23) is turned away from the substrate binding pocket, in the $P6_5$ structure the Met-20 loop blocks the pocket and protrudes into the cofactor binding site. In this respect, the $P6_5$ structure is unique. Additionally, positioning of a Ca^{2+} ion (a component of the crystallization medium) is different in the two crystal packings: in the $P6_1$ structure it lies at the boundary between the two molecules of the asymmetric unit, while in $P6_5$ it coordinates two water molecules, the hydroxyl group of an ethanol molecule, and the backbone carbonyl oxygens of Glu-17, Asn-18, and Met-20. The Ca^{2+} ion thus stabilizes a single turn of 3_{10} helix (residues 16−18 in the Met-20 loop), a second unique feature of the $P6_5$ crystal structure. The disposition of the N5-formyl group in these structures indicates formation, at least half of the time, of an intramolecular hydrogen bond between the formyl oxygen and O4 of the tetrahydropterin ring. This observation is consistent with the existence of an enol−keto equilibrium in which the enolic tautomer is favored when a hydrogen-bond acceptor is present between O4 and N5. Such would be the case whenever a water molecule occupies that site as part of a hypothetical proton-relay mechanism. Two arginine side chains, Arg-52 in the $P6_5$ structure and Arg-44 in molecule A of the $P6_1$ structure, are turned away drastically from the ligand (*p*-aminobenzoyl)glutamic acid moiety as compared with previously reported DHFR binary complex structures. As in the ecDHFR·dideazatetrahydrofolate complex, in both the $P6_1$ and $P6_5$ structures a water molecule bridges pteridine O4 and Trp-22(Nϵ1) with ideal geometry for hydrogen bonding, perhaps contributing to the slow release of 5,6,7,8-tetrahydrofolate from the enzyme−product complex. When either the $P6_1$ or the $P6_5$ structures are superimposed with the NADPH holoenzyme [Sawaya, M. R. (1994) Ph.D. Dissertation, University of California, San Diego], we find that the distances between the nicotinamide C4 and pteridine C6 and C7 are very short, 2.1 and 1.7 Å in the $P6_1$ case and 2.0 and 1.4 Å in the $P6_5$ case, perhaps in part explaining the more rapid release of tetrahydrofolate from the enzyme−product complex when NADPH is bound.

Dihydrofolate reductase (DHFR)[1] catalyzes the reduction of 7.8-dihydrofolate to 5,6,7,8-tetrahydrofolate (THF) by the coenzyme NADPH. DHFR plays a vital role in the metabolism of proliferating cells because it is required for the maintenance of an adequate level of fully reduced folate, which is in turn essential to one-carbon metabolism. Several inhibitors of DHFR are clinically useful drugs; examples are methotrexate (MTX), trimethoprim, and pyrimethamine. With the aim of understanding the molecular mechanism of

[†] Supported by NIH grant CA 17374 to J.K.

[‡] Coordinates of the $P6_1$ and $P6_5$ ecDHFR·folinic acid structures have been deposited in the Brookhaven Protein Data Bank under filenames 1JOL and 1JOM, respectively.

* Corresponding author.

[§] Present address: Department of Physics, Sang-Ji University, Wonju, S. Korea, 220-702.

[||] Present address: Department of Molecular Biology, MB13, The Scripps Research Institute, 10666 N. Torrey Pines Rd., La Jolla, CA 92037.

[⊗] Abstract published in *Advance ACS Abstracts,* May 15, 1996.

[1] Abbreviations: α_{calc}, calculated phase; α_{obs}, observed phase; ddTHF, 5,10-dideazatetrahydrofolate; DHFR, dihydrofolate reductase; DHF, 7,8-dihydrofolate; ecDHFR, *Escherichia coli* dehydrofolate reductase; F_{calc}, calculated structure factor; F_{obs}, observed structure factor; MTX, methotrexate; NADPH, nicotinamide adenine dinucleotide phosphate, reduced form; pABA, *p*-aminobenzoic acid; pABG, (*p*-aminobenzoyl)-glutamic acid; THF, 5,6,7,8-tetrahydrofolate.

S0006-2960(96)00028-1 CCC: $12.00

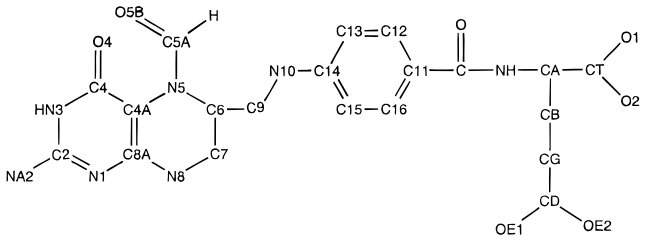

FIGURE 1: Molecular structure and atomic numbering for folinic acid; in ddTHF, N5 and N10 are replaced with C5 and C10, respectively, and the 5-formyl group is not present. The molecule, just like folate, is composed of three segments: the pterin ring (all atoms to the left of C9), the pABA moiety (from N10 to C═O), and the glutamate residue (NH and all atoms to the left of it). The pABA and glutamate moieties together make up the (*p*-aminobenzoyl)glutamate "tail".

DHFR catalysis, our laboratory has carried out numerous studies on the crystal structures of variously liganded complexes of DHFR from *Escherichia coli* (Bolin et al., 1982; Bystroff et al., 1990; Bystroff & Kraut, 1991; Reyes et al., 1995), *Lactobacillus casei* (Filman et al., 1982), bacterial R67 plasmid (Matthews et al., 1986), human (Davies et al., 1990), and chicken liver (McTigue et al., 1992).

We now report the crystal structure of ecDHFR complexed with folinic acid. This structure is of mechanistic interest mainly for two reasons. First, folinic acid is a close analog of the reaction product, THF, differing only by the presence of a formyl group at N5 of the tetrahydropterin ring (Figure 1). Long-standing structural questions concerning the DHFR mechanism relate to THF release: why is this the rate-limiting step under steady-state conditions at physiological pH and why does binding of the next NADPH molecule accelerate THF release (Fierke et al., 1987)? Unfortunately DHFR complexes with THF itself cannot be conveniently studied because THF is easily oxidized by air (Feeney et al., 1981). Unlike THF, however, folinic acid is stable in air under neutral or mildly alkaline conditions (Blakley, 1969).

The second reason for interest in the structure of the folinic acid complex is that its formyl group at N5 may serve as a probe of the surrounding neighborhood. In an earlier model for N5 protonation proposed by this laboratory (Bystroff et al., 1990; Brown & Kraut, 1992), a double proton relay was suggested. It invokes the pteridine O4 as an intermediate proton carrier, requiring an assumption, however, that O4 be enolized, at least transiently. Since the N5-formyl group of bound folinic acid should be near O4 and able to rotate freely, it may interact with O4 and, depending on the latter's tautomeric state, form a hydrogen bond with it. In fact, as described below, this is precisely what occurs in a large fraction of the DHFR molecules within the crystals.

Finally, although unrelated to enzyme mechanistic questions, it is of general interest to note that folinic acid has been used clinically (Bertino, 1977) as an antidote to MTX when the latter is administered in otherwise fatal doses ("leucovorin recue").

MATERIALS AND METHODS

Crystallization. Recombinant ecDHFR was isolated and purified as previously described (Smith & Calvo, 1980, 1982). The concentration and purity of enzyme was determined by its absorbances at 260 and 280 nm. Folinic acid, in the form of its calcium salt, was obtained from Schircks Laboratories (Jona, Switzerland) with a purity of 99%; it is supplied as a 1:1 mixture of 6*R*,α*S* and 6*S*,α*S* diastereoisomers. It is known that the natural diastereoisomer, 6*S*,α*S*, binds to ecDHFR with 10 000-fold higher affinity than the 6*R*,α*S* form (Birdsall et al., 1981). The enzyme was dialyzed against 0.1 M Tris-HCl, pH 7.0 and incubated with a 3-fold molar excess of folinic acid at 4 °C with minimal light exposure for at least 12 h. The complex was then concentrated to about 35 mg/mL using a Centricon-10 protein concentrator (Amicon). Crystals of ecDHFR·folinic acid were grown at 4 °C as follows: 6.25 μL of 0.5 M L-histidine, pH = 6.8, and 6.25 μL of 0.5 M calcium acetate were added to 50 μL of concentrated folinic acid·DHFR complex in an Eppendorf tube, and the mixture was stirred thoroughly. Drops of approximately 5 μL were set up on siliconized cover slips and placed in vapor contact with a reservoir solution containing 18−25% ethanol in 1.0 M Tris-HCl buffer, pH 7.0, at 4 °C. Crystals of good quality and size appeared in 2−3 weeks. As the crystals grew it was apparent that each drop contained crystals of two different gross morphologies, hexagonal bipyramids and hexagonal prisms. The hexagonal bipyramidal crystals, with dimensions 0.5 × 0.3 × 0.3 mm, belong to space group $P6_1$ and are isomorphous with a previously observed crystal form (Bolin et al., 1982), while the hexagonal prisms, with dimensions 0.2 × 0.2 × 1.0 mm, belong to space group $P6_5$, a new one for ecDHFR crystals. After mounting in glass capillaries with a drop of mother liquor, x-ray data were collected at 4 °C using a multiwire area detector (Xuong et al., 1985). The unit cell parameters of both the $P6_1$ and $P6_5$ crystals and data collection statistics are shown in Table 1. Data are 100% complete for both crystal types; the *R*-factors reported are based essentially on all data (all reflections between 20.0 and 1.9 Å). There are two molecules per asymmetric unit in the $P6_1$ crystal and one molecule per asymmetric unit in the $P6_5$ crystal.

Table 1: *E. coli* DHFR·Folinic Acid Complex Crystals: Crystallographic Data Collection and Refinement Statistics

space group	$P6_1$	$P6_5$
no. of molecules per asymmetric unit	2	1
a, *b* (Å)	92.6	96.9
c (Å)	73.1	35.0
R_{sym}[a]	5.8	6.8
Bragg resolution (Å)	2.0	1.9
unique reflections	25 677	15 022
average data redundancy	6.6	7.7
data completeness (%)	100.0	99.7
final *R*-factor,[b] (%)	14.2	14.2
bond length rms deviation (Å)	0.02	0.02
bond angle rms deviation (deg)	3.0	3.0
thermal parameter correlation (Å^2)	5.0	5.0

[a] $R_{sym} = \sum_{khl}(\sum_i|\bar{I} - I_i|/\sum_i I_i)$. [b] R-factor $= \sum_{hkl}|F_o - F_c|/\sum_{hkl} F_o$.

Structure Refinement. Crystallographic refinement of the $P6_1$ structure was carried out as described by Reyes et al. (1995) for other binary ecDHFR complexes in the same space group.

Since ecDHFR has not previously been crystallized in $P6_5$, it was necessary to apply the molecular replacement method to determine its structure. We used XPLOR, version 3.1 (Brünger, 1992), which includes the cross-rotation function, translation search program, and the generalized molecular replacement technique based on Patterson correlation (PC)

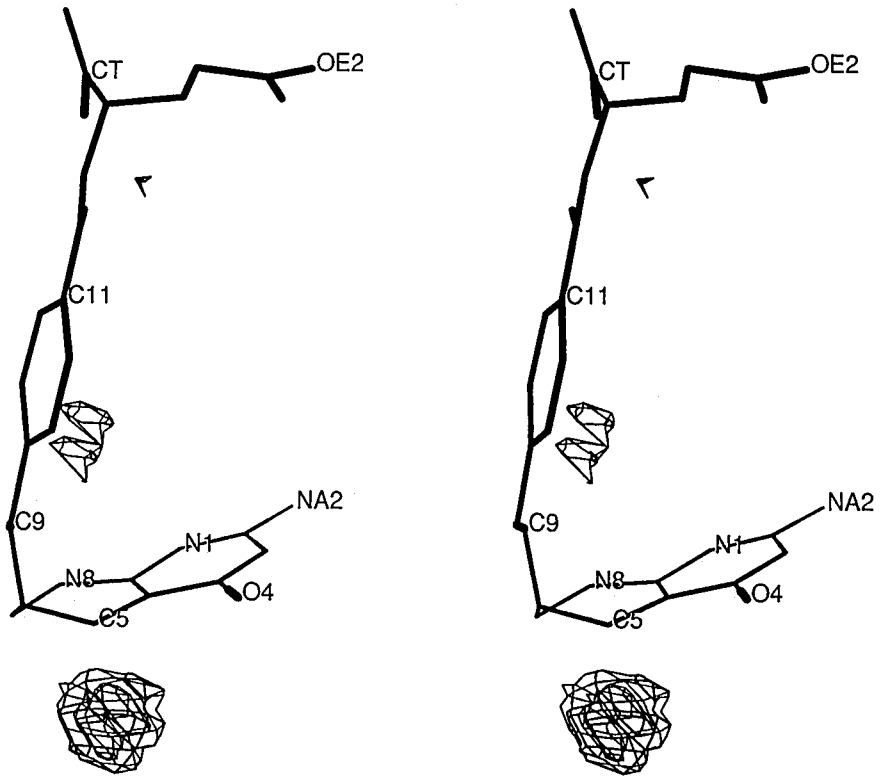

FIGURE 2: $F_{obs}(P6_1$ folinic acid$) - F_{obs}$(ddTHF) electron density map at 4σ contour level showing strong positive electron density corresponding to the 5-formyl group of the ligand, folinic acid, near the pteridine ring (foreground). The ligand model shown is that of ddTHF. The residual positive density near the model's pABA ring is likely due to the small dihedral angular separation between the respective pABA rings of ddTHF and folinic acid (see text).

refinement. The search model was molecule A of the ecDHFR·dihydrobiopterin complex (Reyes et al., manuscript to be submitted), with the ligand omitted. Reflections between 15.0 and 4.0 Å were included in the rotation search, with a maximum Patterson vector of 45 Å. PC refinement was carried out using the highest peaks of the rotation function, after which the translation search was performed in the *x* and *y* directions using reflections between 8.0 and 3.5 Å. Since the position of the unit-cell origin along the *z*-axis is arbitrary in $P6_5$, we chose a molecular position such that all atomic *z* coordinates are positive. This procedure yielded an *R*-factor of 44.0%. We then performed rigid-body refinement, which lowered the R-factor to 39.4%. To further improve the model, we also ran the simulated annealing program in XPLOR, which brought the *R*-factor down to 31.5%. All subsequent steps followed standard procedures for the XPLOR crystallographic refinement package. Finally, the folinic acid ligand was modeled into positive density in the $F_{obs}-F_{calc}$ map and further refinement was carried out using the TNT Refinement Program Package, version 4-C (Oregon State Board of Higher Education, 1991), including all reflections between 20.0 and 1.9 Å. This procedure dropped the *R*-factor from 26.9% to 18.7%.

In the $P6_1$ structure, visual analysis of the conformation of the ligand indicated that it is exclusively the expected 6*S*,α*S* diastereoisomer. The presence of a 5-formyl group was verified by inspection of a difference Fourier calculated with coefficients [$F_{obs}(P6_1$ folinic acid$) - F_{obs}$(ddTHF)] and phases from the refined 2.0-Å structure of the ecDHFR·ddTHF complex (Reyes et al., 1995). The expected positive peak (4σ) of correct shape and size is clearly evident near N5 of the pteridine ring (Figure 2).

In the $P6_5$ structure the presence of the formyl group was confirmed by inspection of an $F_{obs}-F_{calc}$ "omit map" calculated with F_{calc} obtained after removing the formyl group and further refining to minimize residual bias. A strong positive peak next to the pteridine N5 was interpreted as the formyl group. However, it was noticed after further refinement that there always remained a persistent residual positive electron density very close to the formyl oxygen, much too close to be interpreted as a water molecule. When the formyl oxygen was moved into the residual density, however, new positive density appeared where that atom had originally been; and repeated switching of the oxygen position followed by refinement always produced the same result, namely, residual adjacent positive density. It thus became obvious that there must be an appreciable degree of discrete disorder in the ligand. An expanded coordinate set was therefore introduced to represent the ligand, consisting of two partially occupied folinic acid molecules with their formyl groups in the two alternative orientations. They were assigned occupancies of 0.8 and 0.2, respectively, based on their relative electron densities. Further refinement resulted in two coordinate sets representing folinic acid in very similar positions and conformations except that their formyl groups are related by a rotation of approximately 120°. The coordinate set with higher occupancy has its formyl oxygen turned toward, and close to, pteridine O4. The probable significance of this observation is addressed in the Results and Discussion section below.

TNT refinement of both structures, including the formyl group, with iterative cycles of model rebuilding and least-squares minimization was carried to convergence. Water molecules were modeled into positive difference density

peaks that were greater than 4σ, within 2.3−3.3 Å of a hydrogen-bonding partner, and with reasonable hydrogen-bonding geometry. Those with refined *B*-factors ≥ 100 Å^2 were omitted. A total of 427 water molecules have been included in the $P6_1$ structure, and 211 in the $P6_5$ structure. Atoms not visible in electron density maps and therefore deleted from the final structure of the $P6_1$ folinic acid structure are the same as those deleted from the MTX complex (Bolin et al., 1982), but with two additional atoms deleted, namely, the ligand Oϵ1 and Oϵ2 in molecule B. In the $P6_5$ structure, all side-chain atoms are visible except Nη1 of Arg-12 and Cδ and Oϵ1 of Gln-146, which have therefore been deleted. For both the $P6_1$ and $P6_5$ ecDHFR·folinic acid structures the mean uncertainty in atomic positions is 0.2 Å as calculated by the method of Luzzati (1952).

Final *R*-factors and other refinement statistics are listed in Table 1. Coordinates of the present $P6_1$ and $P6_5$ ecDHFR·folinic acid structures have been deposited in the Brookhaven Protein Data Bank; their PDB IDCODES are 1JOL and 1JOM, respectively.

Structural Comparisons. The refined ecDHFR·folinic acid structures were compared pairwise with all other ecDHFR complexes. Small differences in relative rotations of the major and minor subdomains (residues 1−37 and 89−159 and residues 38−88, respectively) were quantified by least-squares superimpositions of backbone α carbon atoms in the separate subdomains using both OVERLAY (TNT package) and INSIGHT II (version 2.2.0, Biosym Technologies, San Diego, CA). Relative subdomain rotations were further characterized with respect to which are more open and which more closed by use of distance difference plots such as that employed by Bystroff and Kraut (1991).

RESULTS AND DISCUSSION

Temperature Factors and Local Disorder. The $P6_5$ structure has appreciably lower B-factors than either molecule of the $P6_1$ structure. The average atomic B-factor in the $P6_1$ structure is 26.7 Å^2 (average over molecules A and B), while it is 18.7 Å^2 in the $P6_5$ complex. The folinic acid in the $P6_1$ complex has an average B-factor of 20.5 Å^2 (average over molecules A and B), while this value is 11.0 Å^2 in the $P6_5$ complex. Although it is conceivable that only the water molecules and side-chain atoms are more disordered in the $P6_1$ structure than in the $P6_5$ structure, this is evidently not the case: if only α carbons are taken into consideration, the average B-values still are 18.9 Å^2 for the $P6_1$ complex but only 11.1 Å^2 for the $P6_5$ complex. These results suggest that the enzyme molecules are less mobile in the $P6_5$ structure, even though they are slightly less tightly packed, occupying about 5% greater volume per molecule. Perhaps the unique conformation of ecDHFR in the $P6_5$ structure—with its Met-20 loop completely closed over the active-site entrance and stabilized by a hitherto unobserved Ca^{2+} ion (see below)—can account for the difference.

In both the $P6_1$ and $P6_5$ structures the β(FG) loop (residues 117−131; connects the βF strand with the βG strand) is the most disordered portion of the molecule, with average B-factors of about 50 Å^2; such an observation is not surprising, as the β(FG) loop is a surface loop. The terminal carboxylate oxygens, Oϵ1 and Oϵ2, of the glutamate moiety of folinic acid in the B molecule of the $P6_1$ structure refined to unrealistically high temperature factors (∼100 Å^2) and so were deleted. The unusually high temperature factors of these atoms may be ascribed to the fact that the terminal glutamate moiety of folinic acid, like that of folate, is directed toward the external solvent and does not interact with the backbone or any side-chain groups.

General Comparisons among Structures. The overall conformations of both molecules A and B in the $P6_1$ folinic acid complex as compared with the isomorphous $P6_1$ ddTHF complex (Reyes et al., 1995) are essentially identical. That is to say, although the conformation of the Met-20 loop (residues 9−23) differs substantially between molecules A and B, all molecules A in the various $P6_1$ structures look alike, as do molecules B. Similarly, the ligand tetrahydropteridine rings all have the same conformation and can be superimposed (Figure 3).

In the $P6_5$ folinic acid complex, however, the situation is somewhat different. Although once again the overall protein conformation is invariant, in this case the Met-20 loop is "completely closed" over the active-site cavity, unlike any other ecDHFR structures seen so far (see Figure 3; conformations of the Met-20 loop will be further discussed below). Moreover, when the bound tetrahydropterin ring of folinic acid in the $P6_5$ complex is compared with that of the $P6_1$ ddTHF complex, it is evident that although they are quite similar, notably with regard to the ring pucker at C6 and C7, their pteridine rings are not strictly coincident (Figure 4).

Relative Positions of Subdomains. ecDHFR is composed of two subdomains, a major subdomain and a smaller adenosine-binding subdomain. The major subdomain is sequentially discontinuous, consisting of residues 1−38 and 110−159, while the minor subdomain consists of residues 39−109 [Bystroff & Kraut, 1991; revised by M. R. Sawaya (1994)]. In the 35 ecDHFR crystal structures in 9 different crystal packings so far determined, the relative positions of the two subdomains has been observed to vary slightly, resulting in a more "open" or a more "closed" conformation. These are exemplified by the apoenzyme, in space group $P3_121$ (Bystroff et al., 1990), which may be regarded as fully open, and the MTX binary complex, in space group $P6_1$ (Bolin et al., 1982), which may be regarded as fully closed. The open conformation is characterized by widening of the elongated crevice between the αB and αC helices (residues 24−35 and 44−50, respectively, with Cδ2 of Leu-28 in the αB helix and Cγ1 of Ile-50 in the αC helix making the closest mutual approach) by about 1.9 Å, as well as enlargement of the adenosine binding pocket, relative to the closed conformation.

Comparing both molecules of the $P6_1$ folinic acid complex with those of the $P6_1$ MTX complex, it is found that the subdomain separation is only about 0.2 Å wider in the former. That is to say, the folinic acid complex in $P6_1$ is almost fully closed. On the other hand, in the $P6_5$ folinic acid complex the subdomain separation is about 0.9 Å wider than in the $P6_1$ MTX complex. In other words, it is about half open. Thus we can conclude (not surprisingly) that crystal packing could have an important effect on the exact molecular conformation.

Does the nature of the ligand also affect the separation between subdomains? When all the $P6_1$ complexes are compared among themselves, the subdomain separation is found to vary over a range of about 0.7 Å, depending on the

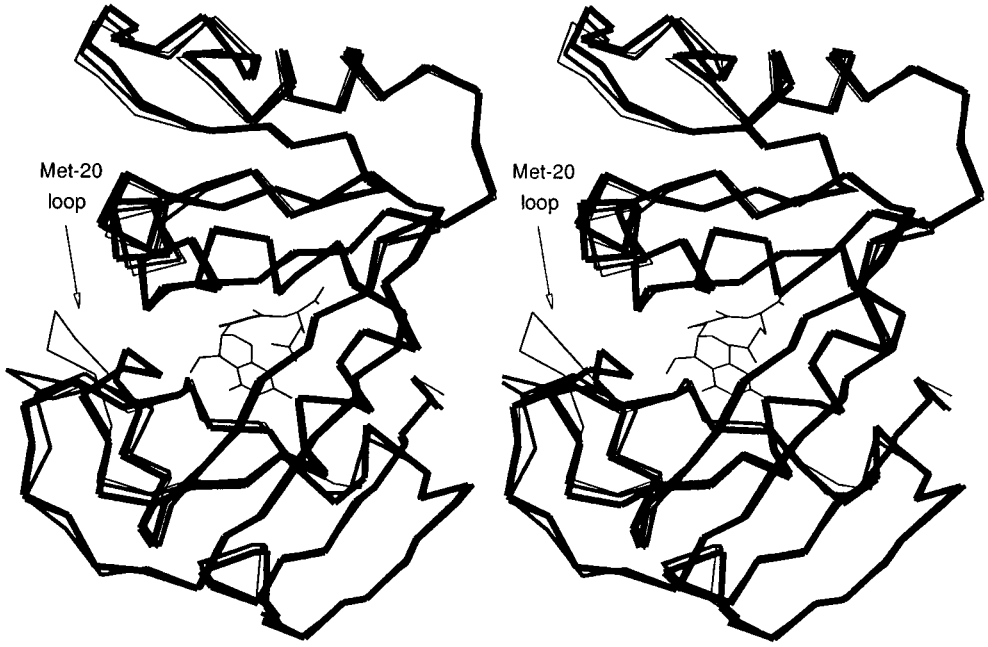

FIGURE 3: Least-squares superimposed α-carbon backbone traces of ecDHFR·folinic acid complexes: (a) thin line, $P6_1$ structure, molecule A; (b) medium line, $P6_1$ structure, molecule B; and (c) thick line, $P6_5$ structure. Their greatly differing Met-20 loop conformations are readily evident in the central left-hand side of the figure (arrow). The ligand model shown (thin lines) is that for folinic acid in molecule A of the $P6_1$ structure.

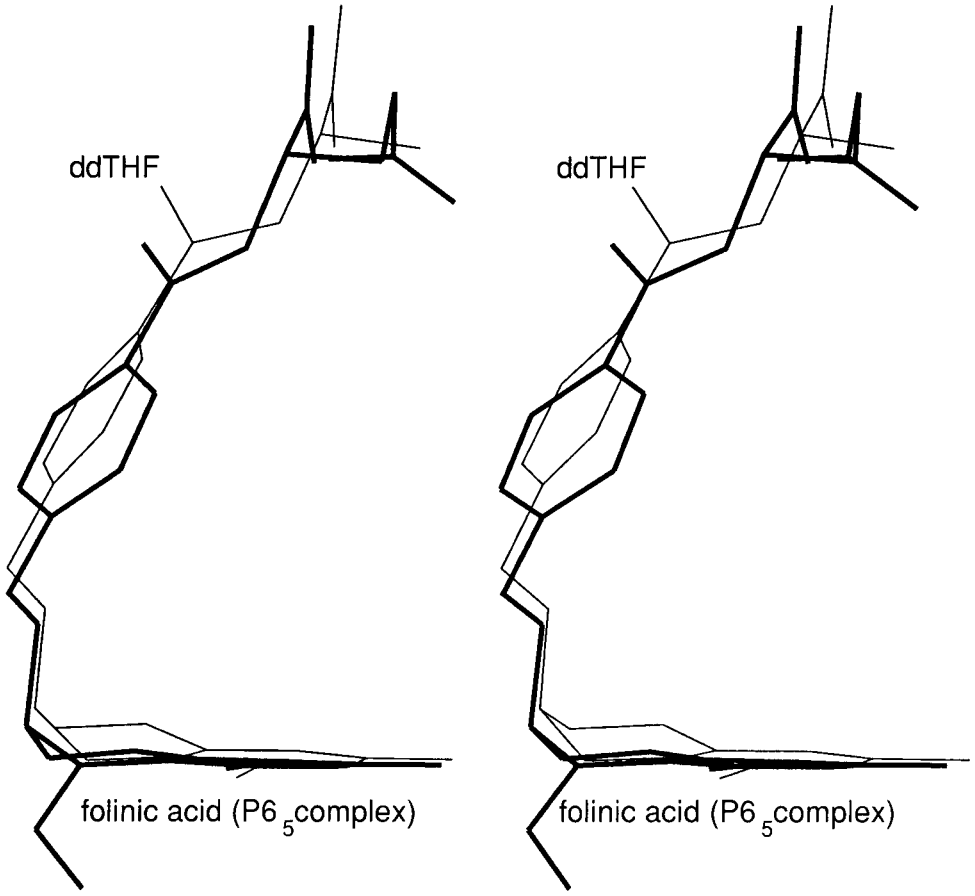

FIGURE 4: Least-squares superimposed structures of the ecDHFR·ddTHF $P6_1$ binary complex (thin line) and folinic acid $P6_5$ binary complex (thick line). The αC atoms of the enzyme were used in the least-squares superimposition, but only the bound ligands are shown. The lateral twist of the pABA ring of folinic acid relative to that of ddTHF is readily apparent. Only the major conformer (80% occupancy) of folinic acid in the $P6_5$ structure is shown; the minor conformer (20% occupancy) is not shown.

ligand. A more complete description and possible mechanistic implications of these observations will be presented in future reports. For the present, however, we note that there appears to be a connection between the detailed binding geometry of the pABA ring and the degree of openness of the intersubdomain crevice. This issue is dealt with below.

Conformations of the Met-20 Loop. Among all the $P6_1$ ecDHFR structures, including the folinic acid complex, molecules A and B differ only in the conformation of their Met-20 loops (residues 9−23). If we consider the Met-20 loop to resemble a planar lid on the entrance to the substrate binding pocket, then in molecule B the pocket is completely open, i.e., the lid makes an angle of roughly 180° with the binding pocket entrance (see Figure 3). In molecule A, on the other hand, the pocket is slightly closed, as the lid is swung toward it by about 15°. In contrst, the $P6_5$ folinic acid complex has a closed Met-20 loop conformation in which the lid lies flat upon the ligand binding pocket orifice (see Figure 3). It appears that the Met-20 loop is able to assume a closed conformation in the $P6_5$ structure because it occupies the empty cofactor binding site. In this respect the $P6_5$ structure is unique among all ecDHFR crystal structures solved to date. The Met-20 loop is prevented from adopting this conformation in the $P6_1$ structure because of crystal packing contacts between molecules A and B of the asymmetric unit. The details of the movement of the Met-20 loop and the various structural factors which influence it will be dealt with in much greater detail in a later publication (Sawaya et al., manuscript in preparation).

Calcium ion is a component of the medium from which both the $P6_1$ and $P6_5$ crystals are grown, and both structures contain a single calcium ion per asymmetric unit. In $P6_1$ the Ca^{2+} ion is located near the βG strand (residues 132−141) and the Met-20 loops of both molecules A and B of the asymmetric unit. However, in $P6_5$ the Ca^{2+} coordinates three backbone carbonyl oxygens in the Met-20 loop [Glu-17(O), Asn-18(O), and Met-20(O)], two water molecules (Wat-246 and Wat-266), and the hydroxyl group of an ethanol molecule (eth-174), also a component of the crystallization medium. It is noteworthy that Asn-18 is the C-terminus of a single turn of 3_{10} helix comprising residues 16−18 of the Met-20 loop. This single helical turn is not observed in any other ecDHFR crystal structure. We believe that interactions between the Ca^{2+} and the Met-20 loop in the $P6_5$ complex help to stabilize the fully closed conformation of the Met-20 loop in that structure.

Position of the Arg-52 and Arg-44 Side Chains. Unexpectedly, the Arg-52 side chain in the $P6_5$ structure is drastically repositioned relative to its location in the $P6_1$ structures, where it is turned toward the carbonyl oxygen of the ligand's glutamate moiety. Although the Arg-52 side chains of molecule A and B in the $P6_1$ structures are similarly positioned, in the $P6_5$ structure it has swung away from the folinic acid by over 6 Å and projects out into the surrounding medium. Thus the distance from the Arg-52 Cζ atom to the glutamate Cα atom is approximately 5 Å in the ddTHF and folinic acid $P6_1$ complexes (both molecules A and B), but this distance is almost 11 Å in the $P6_5$ folinic acid complex.

Additionally, in molecule A of the $P6_1$ folinic acid complex structure the Arg-44 side chain is turned away by about 4 Å from the pABA moiety as compared to its position in molecule B or in either molecule A or B of the other ecDHFR $P6_1$ binary complexes.

It may be useful at this point to summarize certain features of the two folinic acid complex structures we have described here: (a) In the $P6_5$ structure the Met-20 loop is completely closed, the formyl O and pteridine O4 are fully H-bonded (see below), and Arg-52 swings 11 Å away from ligand pABG tail; (b) in molecule A of the $P6_1$ structure the Met-20 loop is partially open, the formyl O and pteridine O4 are only weakly H-bonded, and Arg-44 swings 4 Å away from the ligand pABA moiety; and (c) in molecule B of the $P6_1$ structure the Met-20 loop is completely open, the formyl O and pteridine O4 are *not* H-bonded, and neither arginine side chain in the enzyme swings away.

What are the mechanistic implications of these seemingly correlated structural repositionings? It is possible that the above coordinated movements of the Met-20 loop, the Arg-44 and Arg-52 side chains, and the degree of enolization of pteridine O4 (as evidenced by the H-bond length between it and the formyl oxygen) are physically linked; however, the mechanism of such a linkage is unclear. Thus the simplest explanation is that intermolecular packing differences between the $P6_1$ and $P6_5$ structures are responsible for the variability in the Arg-52 and Arg-44 positions, once again emphasizing the great caution which must be exercised when making detailed molecular comparisons across different crystal packing geometries.

Geometry of Bound Folinic Acid. The most significant new information to emerge from the two crystal structures of the ecDHFR·folinic acid binary complex concerns the N5-formyl group. Quite clearly its carbonyl oxygen hydrogen-bonds with O4 in at least half of the molecules (or at least half of the time). Specifically, in the $P6_1$ structure the formyl oxygen is turned toward O4 in molecule A of the asymmetric unit, while it is turned away from O4 in molecule B. In the molecule where the formyl oxygen is turned toward O4, the distance between the two is 3.4 Å, sufficiently short to imply weak hydrogen bonding. Neither molecule of the asymmetric unit shows any evidence of disordering of the formyl group's orientation (Figure 5). In contrast, however, the formyl group in the $P6_5$ structure apparently can rotate into two different positions, about 120° apart, with occupancies of roughly 0.8 and 0.2. Accordingly, crystallographic refinement was carried forward with two independent folinic acid molecules, appropriately weighted, in the binding site. The final coordinates show that in the predominant binding geometry the formyl oxygen is also turned toward O4, in this case with a distance between the two atoms of 2.8 Å, once again indicating the existence of a hydrogen bond. In the minor binding geometry, the formyl oxygen is turned away from O4 (see Figure 6). The hydrogen in question—that which bridges O4 and O5B in molecule A of the $P6_1$ structure and in the major conformer of the $P6_5$ structure—is *not* visible in the electron density map and has to be simply assumed to exist somewhere between O4 and O5B, forming a nonplanar, irregular ring system with ligand atoms C5A, N5, C4A, C4, O5B, and O4 (see Figure 7a).

It should also be noted that in Figure 6 the two ligand conformers in the $P6_5$ structure appear to differ in their pteridine ring pucker and pABG positioning. It is possible that hydrogen bonding between pteridine O4 and formyl O5B causes the tetrahydropterin ring to assume a somewhat different geometry as compared to the ring geometry when the pteridine O4 and formyl O5B do not interact. Such is also observed on comparing molecules A and B of the $P6_1$ structure: in addition to the differing formyl oxygen orientations of the folinic acid ligands, they differ as well in their tetrahydropterin ring pucker and precise pABG positioning (Figure 5). These relative movements are similar to, although significantly less dramatic than, those observed

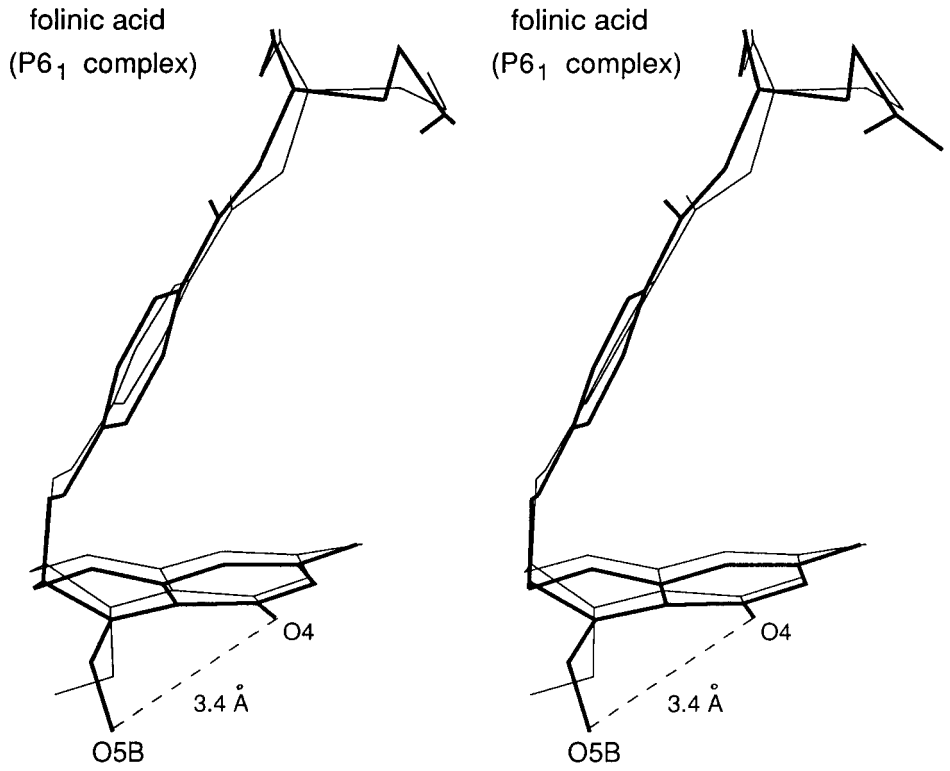

FIGURE 5: Least-squares superimposed structures of the two molecules of the asymmetric unit of the ecDHFR·folinic acid $P6_1$ binary complex: thick line, molecule A; thin line, molecule B. The distance of 3.4 Å between pteridine O4 and the formyl oxygen O5B in molecule A, suggesting a marginal H-bond, is indicated.

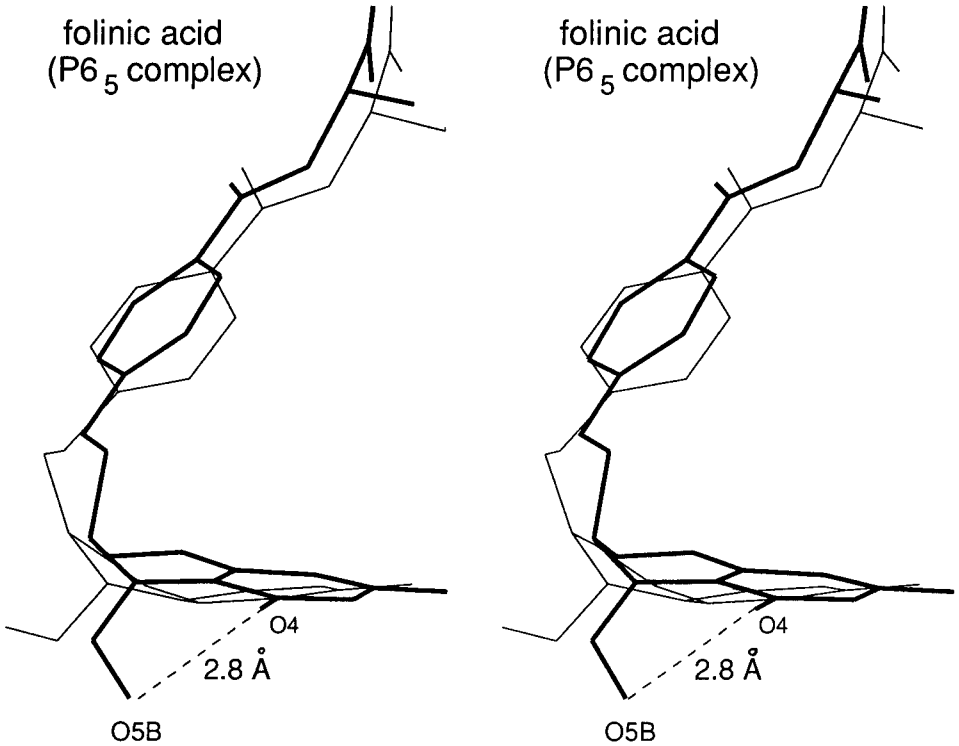

FIGURE 6: Two different positions of the bound folinic acid in the $P6_5$ complex: thick lines, position 1 with 80% of occupancy; and thin lines, position 2 with 20% occupancy. In position 1 the distance between pteridine O4 and formyl oxygen O5B of 2.8 Å, strongly suggesting a hydrogen-bonded interaction, is indicated.

between the major and minor ligand conformers in the $P6_5$ structure (Figure 6), which is perhaps to be expected since the H-bonding between pteridine O4 and formyl O5B is stronger in the major conformer in the $P6_5$ structure than in molecule A of the $P6_1$ structure. Nevertheless, in assessing this apparent slight difference between the major (80% occupied) and minor (20% occupied) ligand conformations in the $P6_5$ structure, it should be kept in mind that crystallographic refinement of the coordinates of the minor conformer will be much less reliable than the others. Thus we are reluctant to place too much emphasis on the accuracy of the minor conformation.

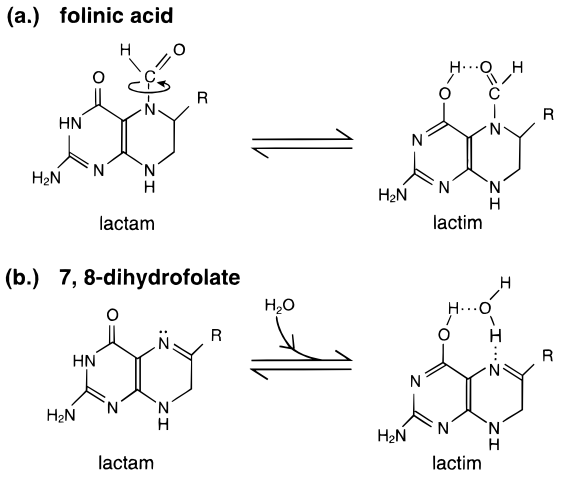

FIGURE 7: Schematic diagram illustrating the promotion of enolization of pteridine O4 by the formyl oxygen in the case of folinic acid (panel a) and by a transient water molecule in the case of DHF (panel b). **R** represents the pABG moiety in both cases. In panel a, the freely rotating formyl group is thought to induce enolization of pteridine O4 when the former's oxygen atom lies proximal to the latter, leading to the formation of an intramolecular H-bond between the two oxygen atoms. In panel b, a transient water molecule enters the active site, perhaps facilitated by the opening of the Met-20 loop; this water eventually H-bonds to pteridine N5 and occupies nearly the same, but probably not identical, position as the formyl oxygen in folinic acid when the latter lies proximal to pteridine O4, inducing enolization of O4 in a similar way. Previous studies (McTigue et al., 1992; Reyes et al., 1995) have strongly established the existence of such a water molecule.

The foregoing strongly suggests the existence of an equilibrium between the lactim (enol) and lactam (keto) tautomers of the 5-formyltetrahydropteridine ring—if not in solution, then certainly when it is bound to the enzyme molecule in the crystal (see Figure 7b). Consequently, since the transition state for dihydrofolate reduction must involve a pteridine ring in a state that is, roughly speaking, sterically and electronically intermediate between dihydro and tetrahydro, it is reasonable to suppose that a similar keto−enol equilibrium might also pertain in the transition state. This idea is made still more attractive by the realization that in the transition state an alternative hydrogen-bond acceptor, namely, a water molecule, probably occupies the space taken up here by the N5-formyl group, bridging O4 and N5. In fact, the presence at this position of a potential hydrogen-bond acceptor, be it a formyl oxygen or a water molecule, should favor the enol tautomer. Panels a and b of Figure 7 together illustrate the above ideas.

These observations are consistent with an earlier proposal for the mechanism of pteridine N5 protonation of DHF by ecDHFR [see Figure 6 in Bystroff et al. (1990) and Figure 3 in Brown and Kraut (1992)]. That proposal involved enolization at O4, at least transiently, promoted by a protonated catalytic-site Asp-27, and the introduction, at least transiently, of an additional proton-relaying water molecule between O4 and N5. Some degree of credibility has now been lent to the latter aspect by the identification of just such a bound water molecule between O4 and N5 in the crystal structure of the ecDHFR·folate binary complex (Reyes et al., 1995). However, the roles of Asp-27 and of O4 enolization have been called into question recently by conflicting observations (Blakley et al., 1993; Cheung et al., 1993; Chen et al., 1994; Basran et al., 1995). In our view the protonation state of Asp-27 and the nature of the N5-protonation mechanism remain intriguingly obscure.

A second curious aspect of the folinic acid geometry concerns the angular twist of the bound pABA ring, which differs appreciably between the $P6_1$ and the $P6_5$ structures. In order to simultaneously compare the three structures, $P6_1$ ecDHFR·ddTHF, $P6_1$ ecDHFR·folinic acid, and $P6_5$ ecDHFR·folinic acid, we performed least-squares superimpositions between each of them and the previously reported $P6_1$ ecDHFR·MTX structure, which served as a fixed reference. Examining the pABA rings in both the A and B molecules, we note that while those of the $P6_1$ folinic acid and ddTHF complexes are essentially parallel (although not coincident, as they are separated laterally by about 0.5 Å), in the $P6_5$ folinic acid complex the ring is twisted by 15° about an axis passing through C11 and C14 (Figure 4). The direction of twist is such that the pABA ring atoms C12 and C13 in the $P6_5$ complex are swung toward the αC helix, while atoms C15 and C16 are swung in the opposite direction, toward the αB helix. This ring twist is accompanied by movement of the αB and αC helixes away from the pABA ring by about 0.3 and 1.5 Å, the precise extent of movement depending on the degree of twist. Since αB is in the major subdomain while αC is in the minor subdomain, it appears that the pABA ring twist is correlated with the large relative subdomain movement observed in the $P6_5$ structure, mentioned earlier. The functional significance, if any, of this dynamic coupling is not clear. Such lateral twisting of the pABA ring has also been observed in a recent structure of GAR transformylase complexed with a folate-derived inhibitor (Klein et al., 1995). It is clear, therefore, that the pABA ring of folate or its variants has the ability to rotate relatively freely.

Implications for Release of THF from the Enzyme−Product Complex. We have proposed recently that puckering of the ecDHFR-bound tetrahydropteridine ring, as seen in the ddTHF complex, brings pteridine O4 closer to Trp-22 so that a conserved, bound water molecule now makes a stronger H-bonded bridge between the two moieties, thereby contributing to slower release of product as compared with reactant [see Figure 6 in Reyes et al. (1995)]. With respect to this particular feature, the geometries of the $P6_1$ and $P6_5$ folinic acid complexes are indistinguishable from one another and very close to that of the ddTHF complex. Thus these two new structures lend further support to the proposal of Reyes et al. (1995).

Additionally, when the NADPH holoenzyme complex (space group $P3_221$; Sawaya, 1994) and the ddTHF complex ($P6_1$) were superimposed, it was found that the enzyme favors an extremely short approach distance of 2.1 Å between pteridine C6 and nicotinamide C4, or 1.8 Å between pteridine C7 and nicotinamide C4 [see Figure 5 in Reyes et al. (1995)]. Applying the same procedure to the $P6_1$ and $P6_5$ folinic acid complex structures gives the same result. In the case of the $P6_1$ structure, the approach distances are the same as for the ddTHF, within 0.1 Å, as expected since the latter is isomorphous in the same $P6_1$ space group. For the $P6_5$ complex, however, the approach distances may be even a little shorter: the C7 to C4 distance is 1.4 Å as compared with 1.8 Å for the ddTHF. These findings strengthen our previous conclusions, based on the crystal structure of the ecDHFR·ddTHF $P6_1$ binary complex, that acceleration of THF release from the enzyme−product complex by binding

a new molecule of NADPH is due in part to a sterically crowded interaction between the product pteridine C7 and NADPH nicotinamide C4.

ACKNOWLEDGMENT

We thank Dr. Michael R. Sawaya for many enlightening discussions and for important advice on protein purification, the collection of crystallographic data, and refinement. We also thank Dr. Ying Su for expert tutorial in the use of the crystallographic program XPLOR, version 3.1.

REFERENCES

Basran, J., Casarotto, M. G., Barsukov, I. L., & Roberts, G. C. K. (1995) *Biochemistry 34*, 2872−2882.

Bertino, J. R. (1977) *Semin. Oncol. 4*, 1977.

Birdsall, B., Burgen, A. S. V., Hyde, E. I., Roberts, G. C. K., & Feeney, J. (1981) *Biochemistry 20*, 7186−7195.

Blakley, R. L. (1969) in *The Biochemistry of Folic Acid and Related Pteridines*, North-Holland Publishing Co., Amsterdam.

Blakley, R. L., Appleman, J. R., Freishiem, J. H., & Jablonsky, M. J. (1993) *Arch. Biochem. Biophys. 306*, 501−509.

Bolin, J. T., Filman, D. J., Matthews, D. A., Hamlin, R. C., & Kraut, J. (1982) *J. Biol. Chem. 257*, 13650−13662.

Brown, K. A., & Kraut, J. (1992) *Faraday Dis. 93*, 217−224.

Brünger, A. T. (1992) in *X-PLOR, version 3.1, A System for X-Ray Crystallography and NMR*, pp 233−269, Yale University Press, New Haven, CT, and London.

Bystroff, C., & Kraut, J. (1991) *Biochemistry 30*, 2227−2239.

Bystroff, C., Oatley, S. J., & Kraut, J. (1990) *Biochemistry 29*, 3263−3277.

Chen, Y.-Q., Kraut, J., Blakley, R. L., & Callender, R. (1994) *Biochemistry 33*, 7021−7026.

Cheung, H. T. A., Birdsall, B., Frenkiel, T. A., Chau, D. D., & Feeney, J. (1993) *Biochemistry 32*, 6846−6854.

Davies, J. F., II, Delcamp, T. J., Prendergast, N. J., Ashford, V. A., Freisheim, J. H., & Kraut, J. (1990) *Biochemistry 29*, 9467−9479.

Feeney, J., Birdsall, B., Albrand, J. P., Roberts, G. C. K., Burgen, A. S. V., Charlton, P. A., & Young, D. W. (1981) *Biochemistry 20*, 1837−1842.

Fierke, C. A., Johnson, K. A., & Benkovic, S. J. (1987) *Biochemistry 26*, 4085−4092.

Filman, D. J., Bolin, J. T., Matthews, D. A., & Kraut, J. (1982) *J. Biol. Chem. 257*, 13663−13672.

Klein, C., Chen, P., Arevalo, J. H., Stura, E. A., Marolewski, A., Warren, M. S., Benkovic, S. J., & Wilson, I. A. (1995) *J. Mol. Biol. 249*, 153−175.

Luzzati, V. (1952) *Acta Crystallogr. 5*, 802−810.

Matthews, D. A., Smith, S. L., Baccanari, D. P., Burchall, J. J., Oatley, S. J., & Kraut, J. (1986) *Biochemistry 25*, 4194−4204.

McTigue, M. A., Davies, J. F., II, Kaufman, B. T., & Kraut, J. (1992) *Biochemistry 31*, 7264−7273.

Reyes, V. M., Sawaya, M. R., Brown, K. A., & Kraut, J. (1995) *Biochemistry 34*, 2710−2723.

Sawaya, M. R. (1994) Ph.D. Dissertation, Department of Chemistry and Biochemistry, University of California, San Diego, La Jolla, CA.

Smith, D. R., & Calvo, J. M. (1980) *Nucleic Acids Res. 8*, 2255−2274.

Smith, D. R., & Calvo, J. M. (1982) *Mol. Gen. Genet. 187*, 72−78.

Tronrud, D. E., Ten Eyck, L. F., & Matthews, B. W. (1987) *Acta Crystallogr. A43*, 489−501.

Xuong, N. H., Nielsen, C. P., Hamlin, R., & Anderson, D. H. (1985) *J. Appl. Crystallogr. 18*, 342−350.

BI960028G